Granular Jamming Feet Enable Improved Foot-Ground Interactions for Robot Mobility on Deformable Ground

Shivam Chopra, Michael T. Tolley and Nick Gravish

***Abstract*—Recent studies on dynamic legged locomotion have focused on incorporating passive compliant elements into robot legs which can help with energy efficiency and stability, enabling them to work in wide range of environments. In this work, we present the design and testing of a soft robotic foot capable of active stiffness control using granular jamming. This foot is designed and tested to be used on soft, flowable ground such as sand. Granular jamming feet enable passive foot shape change when in contact with the ground for adaptability to uneven surfaces, and can also actively change stiffness for the ability to apply sufficient propulsion forces. We seek to study the role of shape change and stiffness change in foot-ground interactions during foot-fall impact and shear. We have measured the acceleration during impact, surface traction force, and the force to pull the foot out of the medium for different states of the foot. We have demonstrated that the control of foot stiffness and shape using the proposed foot design leads to improved locomotion, specifically a $\approx 52\%$ reduced foot deceleration at the joints after impact, $\approx 63\%$ reduced depth of penetration in the sand on impact, higher shear force capabilities for a constant depth above the ground, and $\approx 98\%$ reduced pullout force compared to a rigid foot.**

***Index Terms*—Soft robot applications, biologically-inspired robots, soft robot materials and design, legged robots.**

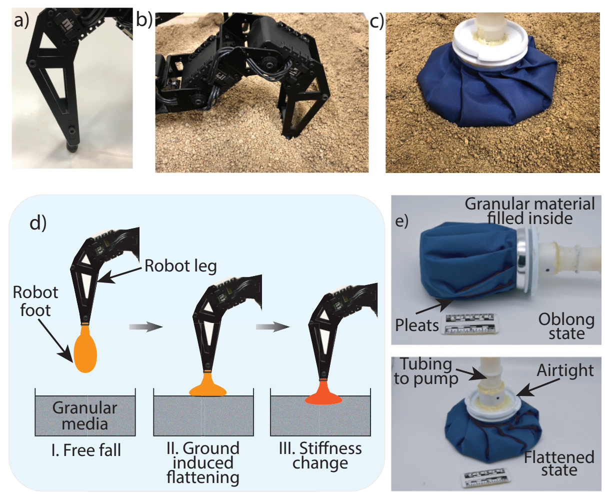

Fig. 1. (a) A foot of a commercially available hexapod robot, (b) Robot foot with pointy end sinking in granular media (plastic beads of 3 mm diameter), (c) The proposed foot in flattened state on sand, (d) Schematic showing the concept of the robot foot which after (I) free fall impacts the granular media and flattens (II) and then jamming is initiated to rigidify (III), (e) The proposed foot design in oblong and flattened state

I. Introduction

Modern technology has created robotic systems that have excellent locomotion performance on flat ground [1]–[3], open water [4], [5] and air [6], [7]. However, robust ground-based mobility in realistic environments with flowable, uneven ground, has seen limited success [8], [9]. Robot mobility requires generating reliable and stable traction forces which are complicated on complex natural terrain like sand and rubble [10].

On the contrary, many terrestrial animals inhabit incredibly complex environments with surfaces such as rubble, leaf litter, sand, mud, snow, and grass that pose high demands on foot placement, joint control, and body control. Particularly, walking on granular media like sand in a desert ($\approx 10\%$ of the Earth's land area) is challenging because it behaves like a fluid-like flowing medium above a yield stress limit [11]. In granular environments, off the shelf legged robots can display poor performance when walking on granular material because rigid, pointed feet may sink into the grains (Fig. 1a). However, with appropriate modifications to mechanical design [12] or control [9], [13] robots can perform well on granular media but the performance is highly sensitive to the packing fraction and the limb kinematics of the robot as the yield strength of granular medium increases with the increase in packing fraction [14].

Strategies to improve legged robot performance on granular substrates have included decreasing the size and weight of the robot [15] to mitigate foot penetration, alteration of legged gait cycle [9], and using limbless robots to improve contact area [8]. The use of feet that change shape passively is another potential strategy that may improve locomotion performance on sandy surfaces [16], [17]. Many works have been published on adaptable feet by increasing the number of contact points per foot [18] and biomimetic foot mechanisms [19]–[21]. From a bio-inspired perspective, animals like camels and elephants have thick footpads (digital cushions) allowing them to distribute forces during bearing weight and to store or absorb mechanical forces [22]. Further, in the case of camels, the

Manuscript received: October 15, 2019; Revised February 6, 2020; Accepted March 4, 2020.

This paper was recommended for publication by Editor Cecilia Laschi upon evaluation of the Associate Editor and Reviewers' comments. *This work was funded by NSF EAGER Grant 1837662

All authors are with Department of Mechanical and Aerospace Engineering, University of California San Diego, 9500 Gilman Dr, La Jolla, CA 92093 USA s7chopra@eng.ucsd.edu, tolley@ucsd.edu, ngravish@eng.ucsd.edu (Corresponding author: Nick Gravish)

Digital Object Identifier (DOI): see top of this page.

footpads are filled with fat which may keep them from sinking into the soft desert sand. The efficiency of footpads for animal locomotion in deserts serve as a motivation for this work. We hypothesize that a passively shape changing and actively stiffness changing foot can aid in improved locomotion on granular media.

Adaptable foot designs using granular jamming have been proposed for better locomotion on rough terrain [23]–[25], but these have not been designed or tested on deformable ground such as granular media. Granular jamming is the phenomena in which an enclosed collection of granular material (coffee grounds, glass beads, etc.) stiffen (jam) when put under negative pressure. In previous work, it was shown that granular jamming feet, when kept in a loose state, leads to better foot ground contact, and when in an activated (rigid) state leads to better traction during walking [23]–[25]. Although it has been argued that damping in the foot is desirable for a non bouncy behavior [23], a purely soft foot can lead to problems as the propulsion forces from joint actuators do not push the body forward, but instead simply cause the robot leg to slip within the soft foot resulting in no forward motion [20]. Thus, for locomotion it is desirable to have a soft foot to adapt to surfaces, and a stiff foot to allow for generation of proper traction forces [25]. These traction forces are independent of the shape and surface area of contact for traversing on rigid ground but for granular terrain it is desirable for the foot to have least depth of penetration, making surface area of contact and shape of the foot important factors for maximizing the locomotion performance on granular media.

In this work we propose a soft robot foot which flattens up after impact with the medium leading to more surface area causing less penetration and then actively changes stiffness (Fig. 1d) using granular jamming. Rigid body impacts with granular media have been studied in previous works [26] but soft body interactions with granular media under free fall impact and drag haven't been studied, which will be briefly discussed in this work. We performed a series of experiments with the proposed foot design for measuring the efficiency of the robot foot for locomotion in sand by analyzing parameters like peak acceleration at drop, depth of penetration, shear force and pullout force after drop and drag.

II. Foot design

A granular material enclosed by a flexible air tight sheath can exhibit unique stiffness and shape changing behaviors when positive or negative air pressure is applied. When the granular volume is at ambient pressure the grains within can behave like a fluid and thus the volume can change shape easily. However, when a negative pressure is applied to the volume the enclosing sheath applies a pressure inward on the granular material which jam, and the high friction between the grains makes the volume behaves like a solid. This phenomenon is familiar to anyone who has handled a vacuum sealed coffee bag, in the vacuum state the bag is rigid but when the vacuum is released it becomes soft and deformable. This phenomenon has recently been exploited to make adaptable robot grippers [27].

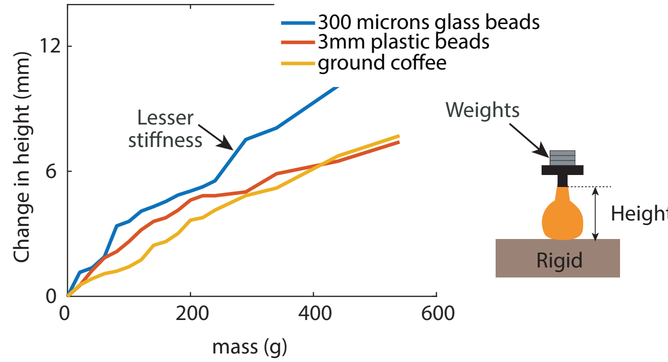

Fig. 2. Experiment to select the filling material for the foot. The plot showing the mass with the change in height from the ground for three different materials and a schematic shows the experimental procedure. The mass is from the weights that are added sequentially

Our proposed foot design was focused on locomotion on granular media (sandy ground). The design was based on a granular jamming foot [25] but in addition to stiffness change, this foot was designed to exhibit shape change on impact. It consisted of an air tight enclosing membrane and a filling material for granular jamming. For the enclosing membrane, we used a commercially available ice pack. The membrane was made of an inelastic textile material with pleats (Fig. 1e) such that on impact with the ground, the membrane would flatten and thus generate a larger surface area in contact, thus leading to less penetration in sand for a given mass of robot. The foot was about 8 cm in diameter in the elongated shape (when not in contact with a surface) and approximately doubled ($13-15$ cm) in cross-sectional diameter when when pressed and flattened against the ground (Fig. 1d-e). We initially performed experiments with a latex membrane but ultimately did not use this material for several reasons. The durability of latex for interaction with complex and rough ground was problematic as it failed quickly. Furthermore, the latex membrane elasticity required a substantially larger fill volume of grains which led to sub-optimal foot shape change abilities when interacting with the granular media. We found that an inelastic, tough textile reminiscent of taffeta was durable yet capable of appropriate shape change.

The filling material selection was based on a quasistatic loading experiment in which the foot was placed on a rigid substrate (wood) and was only free to move vertically. Weights were added on the top sequentially (Fig. 2) and the height of the foot above the ground was measured using pictures from a camera and tracking was done using MATLAB (The MathWorks, Inc.). We chose to test ground coffee, 3 mm diameter plastic beads, and $210-300$ μm diameter glass beads (Potters Industries with density ρ = 2.51 g/cm^3) based on past use in granular jamming and ease of availability [14], [26], [28]. As seen in the plot (Fig. 2) for a given mass on the foot, the change in height of the foot above the ground is highest in case of glass beads because of lesser friction between the glass beads compared to other materials which leads to lesser stiffness of the foot. The filling material was filled up to the brim of the membrane and a tube was attached to the inlet with

This article has been accepted for publication in a future issue of this journal, but has not been fully edited. Content may change prior to final publication. Citation information: DOI 10.1109/LRA.2020.2982361, IEEE Robotics and Automation Letters

a sponge inside for jamming activation using vacuum pump.

III. Experimental procedures

For a robot foot to walk on granular media it is desirable to have minimum peak vertical force on the joints where the foot is attached, minimum depth of penetration in the medium, maximum shear force for forward propulsion in the foot (no slip), and minimum force required to lift the foot out of the medium. To determine how stiffness state of the foot affected these parameters of foot-ground interaction we performed a series of experiments in two groups as follows: 1) foot drop experiments in which we allowed a foot to impact the ground at a realistic velocity, with variable foot stiffness, and 2) shear and pull out experiments in which we measure the foot's shear resistance against the granular surface and the force required to remove the foot. Below we describe these two methods in depth.

A. Granular material testing platform

An air fluidized bed of square cross-section 43 by 43 cm was filled with spherical glass beads of diameter $212-300\ \mu$m (Potters Industries with density ρ = 2.51 g/cm^3) to a depth of 20 cm [Fig. 1(a)]. The floor of the granular testing platform was made of a porous plastic membrane with pore sizes smaller than the particle diameter. The porous floor was supported by an aluminum honeycomb structure with an enclosed volume below. The outflow of a shop vacuum was connected to the volume below the porous floor. The vacuum was 6.5 HP and was connected to wall power source through a proportional relay controlled by an Arduino microcontroller. By varying the voltage of the proportional relay we were able to control the air flow through the granular material. The volume fraction ϕ of the granular media was determined from image-based measurements of the bed height by the equation $\phi = M/\rho A h$, where M, A and h are the the the total mass of the grains, area of the bed, and height of the bed respectively [14]. Before each experiment air flow through the porous membrane initially fluidized the medium [9] and then by slowly ramping down the air flow we got our desired packing fraction ϕ measured as 0.58 ± 0.03 which falls in the range of ϕ of loosely packed sand observed in desert sand dunes [29].

B. Foot drop experiments

For these set of experiments (Fig. 3a), an accelerometer (Analog Devics, ADXL326) was attached to the foot assembly for measuring the acceleration in the vertical direction on impact. The assembly was then fixed with a 3D printed fixture to a bearing setup consisting of two linear bearings and two 12 mm diameter steel shafts oriented vertically and clamped rigidly to the frame. The foot assembly was constrained to move only in the vertical direction and was supported at the base of the foot to inhibit tilting of the whole foot during impact. Further, the foot assembly was attached to a 9.525 mm diameter tube which was connected to a vacuum pump (Kozyvacu TA350), with 0.25 HP power and 3.5 ft^3/min flow rate, controlled by a custom Arduino program using a relay, which pressurises the foot from 100 kPa (soft) to 30 kPa (rigid). A 12 V electromagnet was clamped to the top of the frame and an iron piece was glued to the top of the foot so that it could be held by the magnet at the start of the experiment. The signals from the electromagnet (on/off), the vacuum pump (on/off) and the accelerometer (analog) were recorded at the same sample rate of 4000 Hz through a data acquisition device (National Instruments USB-6001) using a MATLAB program. A high speed camera (Phantom VEO410L) was used to track the trajectory of the drop carriage and the diameter of the foot after impact. For each experiment, the foot was attached to the electromagnet in the soft state (vacuum off) and the bed was fluidized. The data collection started as soon as the electromagnet turned off and the time to turn on the vacuum pump was calculated in reference to the time of impact from the ground for different delay times. All the measurements were taken for free fall of the foot from a height of 30 cm above the ground from the base of the foot corresponding to an impact velocity of ≈ 2.4 m/s.

C. Shear force and pullout experiments

For these sets of experiments, a similar setup as to the previous section was used with some modifications. A horizontal slider with linear bearings was added in addition to the vertical slider such that the foot was free to move horizontally and vertically, as shown in Fig. 5a. A motorized stage (Thorlabs MTS50-Z8) was attached to a 5 kg load cell that displaced the foot in shear through a tension wire. The load cell was connected to a load cell amplifier (FUTEK Inc.) and recorded using a data acquisition system (NI USB-6001) in MATLAB. For every trial, the assembly with the horizontal slider and foot was dropped from a height of 15 cm after fluidizing the granular bed with glass beads. The inelastic string was then affixed to one end to the load sensor and the foot on the other such that the foot could be dragged horizontally using the motorized stage with trajectory controlled using a MATLAB program with a constant velocity of 1 mm/s. The displacement of the foot was tracked using a synchronized camera and a MATLAB program. The experiment was done for four cases of foot states, (1) rigid drop and rigid shear (the vacuum was turned on before drop and remains on for the whole experiment), (2) rigid drop and soft shear (the vacuum was turned on before drop and remained on until drop but turned off for the shear experiment), (3) soft drop and soft shear (vacuum was never on), (4) soft drop and rigid shear (vacuum was turned on after drop).

Further, we directly measured the depth of penetration for all the four cases after dropping from a height of 15 cm using images from the camera. For the rigid drop cases the depth was equal to the change in the height of the foot above the ground as the foot didn't change shape. For the soft drop cases, we assumed that the flattened shape of the foot remained the same when dropped on a rigid surface and on the granular bed. Using this assumption we calculated the depth of penetration (Fig. 6a) for these cases using images from the camera.

After the drag experiment was complete, the foot was pulled out of the granular bed by a force gauge (MARK-10), (Fig. 7a)

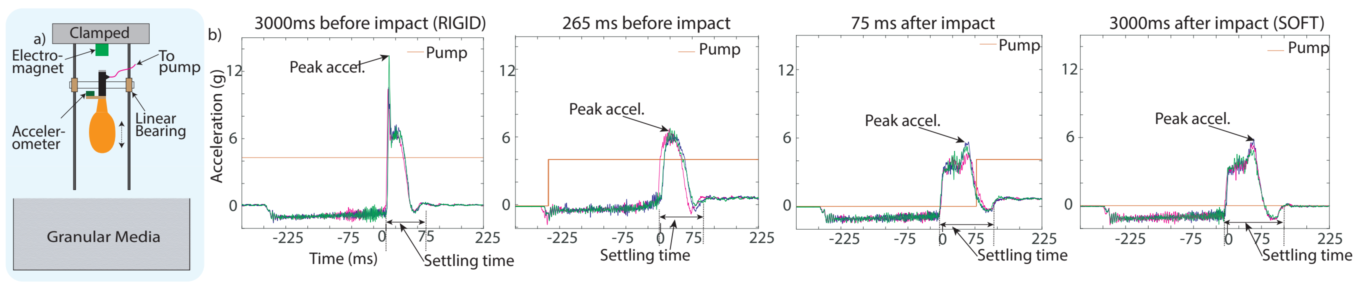

Fig. 3. Dynamics of the foot impacting granular media (a) Experimental setup for drop, (b) Plots showing the acceleration profiles in terms of acceleration due to gravity(g) as soon as the drop starts (3 trials each) for different vacuum turn on times. The time is relative to impact time of the foot (at 0 ms)

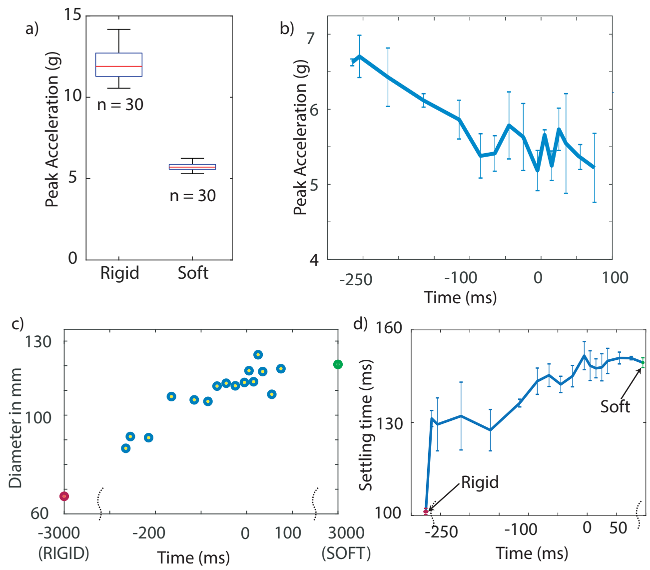

Fig. 4. (a) Bar plots for rigid and soft states of the foot for 30 trials, (b) Peak acceleration for the drop experiment at different time delays of the vacuum pump measured from Fig. 3b, (c) Diameter of the foot above the granular media after impact for different delay times of the pump, (d) Settling time of the foot calculated from Fig. 3b for different delay times.

and the force from the gauge was recorded using a data acquisition software (MESUR$^{\text{TM}}$gauge Plus). For calculating the weight of the foot assembly, the foot was placed on a rigid substrate and then lifted up using the force gauge. The pullout force for all four cases was calculated by subtracting the weight of the assembly from the measured force to lift the whole assembly from the granular media after the drop-and-drag tests.

IV. Results and Discussion

A. Dynamics of foot impacting granular substrate

Fig. 3b shows the acceleration of the foot for four different delay times of the vacuum pump. We chose acceleration to be positive in the direction opposite gravity and acceleration is normalized in terms of acceleration due to gravity (g). In all four plots, the acceleration drops from 0 g to -1 g as soon as the drop occurs. When the foot was dropped as rigid (vacuum on at 3000 ms before impact) on the granular bed there was a sudden increase in the acceleration to 12 ± 1 g and then the acceleration decreased because the foot penetrated the medium and then came back to 0 g as the foot came to rest which matches well with previous work [26]. On decreasing the vacuum delay time to 265 ms before impact, we observed a decrease in the peak acceleration to 5.5 ± 0.5 g and increase in the settling time (time to come to rest) for the foot. Turning on the vacuum after the impact resulted in a reduced peak acceleration (Fig. 4a) and an increase in the settling time until the foot behaved as a completely soft foot with no prominent sudden peak and a slow penetration into the granular bed. The results show that by varying the stiffness state of the foot we can control the peak acceleration of the foot as it comes to rest. Such control may be useful to reduce the jerk on the body when the foot first comes in contact with the ground, in which case an initially soft foot would minimize this rapid change in acceleration.

Using the high speed cameras, we also measured the diameter of the foot above the ground after drop for different pump times (Fig. 4b). For the rigid case the diameter of the foot is the smallest because the foot doesn't change shape. As the vacuum onset time moves closer to the impact time the foot diameter after impact increased until it saturated to a constant value because the foot starts behaving like a completely soft foot as increase in the surface area of the foot leads to lesser penetration depth.

B. Shear force and pullout force measurements

We measured the shear resistance of the foot after impact experiments (Fig. 5). Force versus displacement plots for four different cases of foot state during drop and shear all show a shear force that increases with displacement (Fig. 5b). The force here was measured using the load cell and the displacement of the foot was tracked using the camera during shear test. For the rigid drop followed by rigid shear case, the foot penetrates deeply into the granular medium following impact as seen in Fig. 5c. Because the foot is so deep, and because it is maintained in a rigid state, thus the shear force rises very fast until ≈ 2 mm and then goes on increasing gradually up to 25 N for 30 mm. This continual increase in shear force with displacement is a result of the growing size of a pile of grains in front of the foot which causes an increase in drag. For the rigid drop followed by soft shear, the foot again penetrates deeply into the granular media, however when the vacuum is released and the foot turns soft prior to shear, the

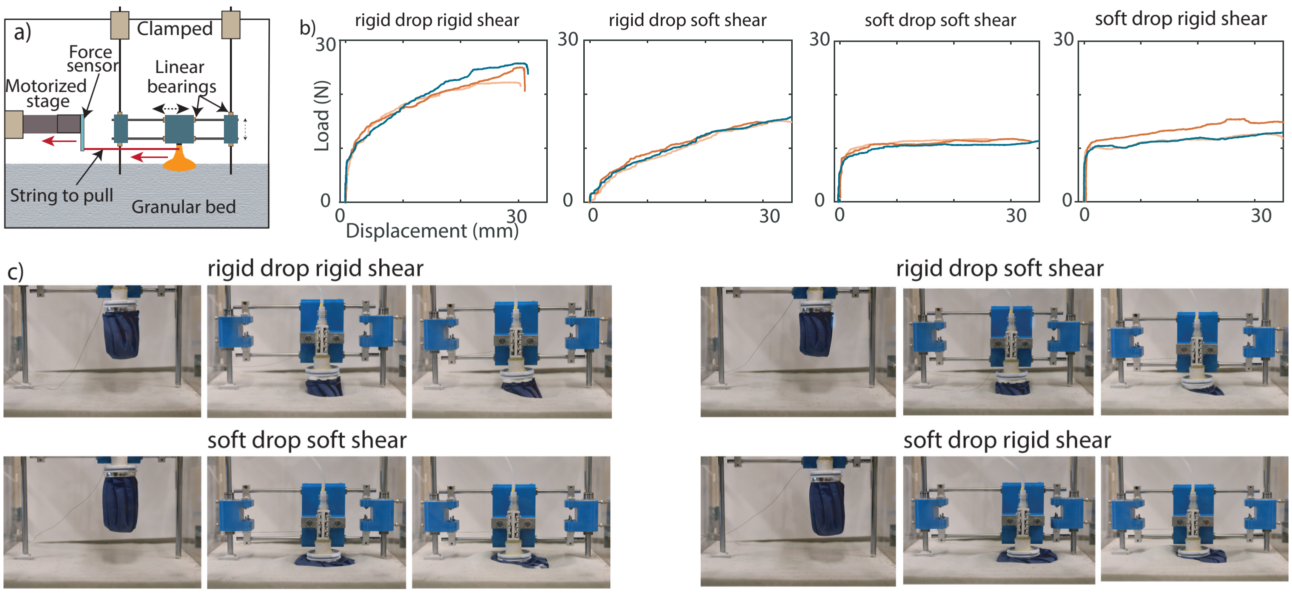

Fig. 5. (a) Experimental setup for shear experiments, (b) plots showing shear force during drag with displacement of the foot for four different states of the foot. 3 trials have been done for each foot state as shown, (c) The snapshots show initial position, after drop and after drag snapshots for the four different conditions of the foot

foot starts to slip within the granular medium causing the shear force to increase more slowly. Similarly to the rigid-rigid case a grain pile forms in front of the foot causing a slow rise in force.

For the soft drop followed by soft shear case, the soft foot impacts the ground and thus is deformed to a flattened shape after coming to rest. Once the foot is dragged the shear force rises very quickly and then saturates at 11 N. Since the flat shape doesn't sink deep into the medium, the pile of grains is substantially smaller in this experiment which causes the shear force to remain relatively constant. Similarly, for the soft drop followed by the rigid shear case, the impact dynamics are the same as previously described with the foot adopting a flattened shape. Upon dragging laterally the shear force rose to a similar value as the soft drop then soft shear case, but in this experiment the shear force has a gradual rise over the full displacement. As can be seen in the snapshots (Fig. 5c), the pile of grains that forms in front of the foot is larger for the rigid dragged foot than the soft dragged foot. This is likely due to the soft foot slipping and deforming within itself. The results indicate that soft drops are optimal for achieving maximum shear force for a given height of the foot above the ground.

The pullout force is highest (Fig. 7b) for rigid drop cases because it goes deep in the granular bed (Fig. 6b) and requires about 10 times more force than the soft drop cases as the soft foot flattens up and doesn't sink in the medium. Pullout force gives us an estimate of how much force would be required to lift up the leg of a robot after a step has been done. As the energy required to lift a rigid foot out of the sand is about 10 times as compared to a soft flattened foot, a soft foot while dropping is more energy efficient for locomotion on granular media.

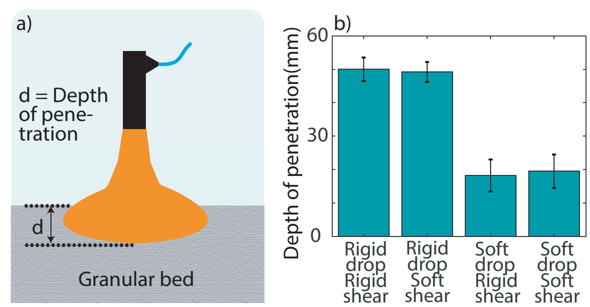

Fig. 6. (a) Schematic showing the depth of penetration d, (b) depth of penetration measured using the camera for the four different cases for 3 trials of experiments

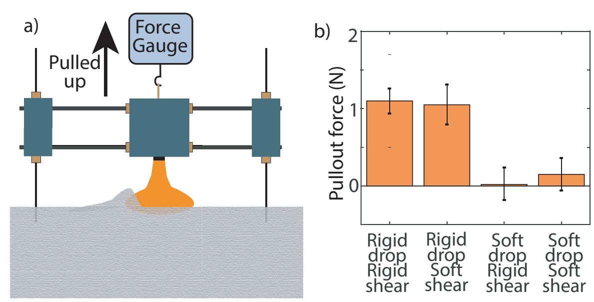

Fig. 7. (a) Schematic showing the pullout force experimental setup (b) Pullout force for the four different cases for 3 trials of experiments

V. Foot performance comparison and selection

We summarize all our results in Fig. 8, where each bar plot has been scaled in reference to the maximum value among the four cases. The shear forces in rigid drops are highest because of the maximum depth of penetration (Fig. 6b). The drag force F_d on a cylinder of diameter D is given by $F_d = \eta \rho g D d^2$ [30], where η characterizes the grain properties (surface friction, packing fraction, etc.), ρ is the density of the glass beads, d is the depth of penetration and g is acceleration due to gravity. Assuming all the parameters to remain the same for these sets of experiments, $F_d = Kd^2$ where K is the drag coefficient. A property of generating traction forces on granular material is that by penetrating deeper in the ground, we can generate more shear force prior to slipping. But this strategy comes at a significant cost as removal of the foot is much harder because of sand pileup and friction, and the effective leg length is shortened because of deeper penetration of the foot. Thus, the drag coefficient K indicates how efficient a foot is in supporting traction force for a constant depth d. We observe that the drag coefficient is highest for soft drop rigid shear along with minimum pullout force. Soft drop states come out to be the most efficient in terms of least depth of penetration and least peak deacceleration at drop. Soft drop rigid shear and soft drop soft shear do not have much difference in performance, however it is desired for a foot to remain rigid during transmission of propulsion forces so that no energy is lost in deformation of the soft foot.

VI. Conclusion

In this work we have proposed a foot design which can passively change shape and actively change stiffness for improved locomotion on granular media. It was shown that the foot in the soft (unjammed) state damped the vertical impact forces (least peak acceleration) and flattened up for an increased contact area and when jamming was initiated the foot turned rigid to become more capable in transmitting horizontal propulsion forces. We have shown that using the foot design with pleats such that it is soft before drop and then rigid during shear led to reduced foot deaccelerations at the joints, lower pullout force, lower depth of penetration and greater drag coefficient at a certain displacement of the foot.

Future directions for this work may include more robophysical testing of the foot by changing the packing fraction of the granular media and by changing the slope of the bed. Future work could test the foot on the legs of the robot walking in desert or beach environment outside the lab thus size of the foot also needs to be scaled down and appropriate control schemes for the vacuum pump would need to to be developed with the gait cycle of the robot

Acknowledgment

This material is based upon work supported by the National Science Foundation under Grant number 1837662. Any opinions, findings, and conclusions or recommendations expressed in this material are those of the author(s) and do not necessarily reflect the views of the National Science Foundation. We would also like to thank Emily Lathrop, Saurabh Jadhav and Philby Wang for their suggestions and contributions to this work.

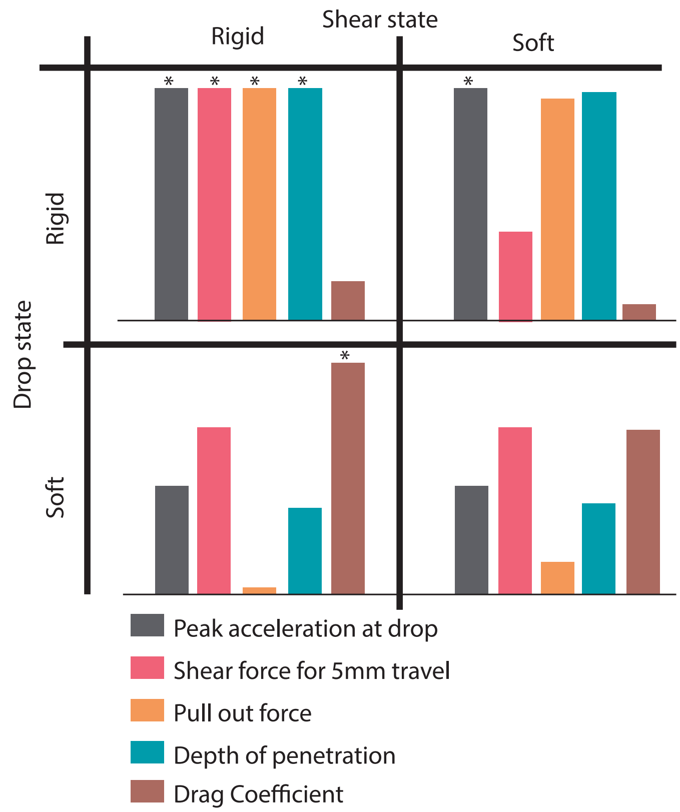

Fig. 8. Summary of results showing the parameters for four different cases of the foot. The plots are not scaled with the real units but scaled with respect to the highest value on each parameter which is shown with an asterisk(*) on top

References

[1] S. Seok, A. Wang, Meng Yee Chuah, D. Otten, J. Lang, and S. Kim, "Design principles for highly efficient quadrupeds and implementation on the MIT Cheetah robot," in *2013 IEEE International Conference on Robotics and Automation*. IEEE, may 2013, pp. 3307–3312. [Online]. Available: http://ieeexplore.ieee.org/document/6631038/

[2] U. Saranli, M. Buehler, and D. E. Koditschek, "RHex: A Simple and Highly Mobile Hexapod Robot," *The International Journal of Robotics Research*, vol. 20, no. 7, pp. 616–631, jul 2001. [Online]. Available: http://journals.sagepub.com/doi/10.1177/02783640122067570

[3] R. Schroer, M. Boggess, R. Bachmann, R. Quinn, and R. Ritzmann, "Comparing cockroach and Whegs robot body motions," in *IEEE International Conference on Robotics and Automation, 2004. Proceedings. ICRA '04. 2004*. IEEE, 2004, pp. 3288–3293 Vol.4. [Online]. Available: http://ieeexplore.ieee.org/document/1308761/

[4] J. M. Anderson and N. K. Chhabra, "Maneuvering and Stability Performance of a Robotic Tuna," *Integrative and Comparative Biology*, vol. 42, no. 1, pp. 118–126, feb 2002. [Online]. Available: http://www.ncbi.nlm.nih.gov/pubmed/21708700 https://academic.oup.com/icb/article-lookup/doi/10.1093/icb/42.1.118

[5] C. Stefanini, S. Orofino, L. Manfredi, S. Mintchev, S. Marrazza, T. Assaf, L. Capantini, E. Sinibaldi, S. Grillner, P. Wallén, and P. Dario, "A novel autonomous, bioinspired swimming robot developed by neuroscientists and bioengineers," *Bioinspiration & Biomimetics*, vol. 7, no. 2, p. 025001, jun 2012.

[6] K. Y. Ma, P. Chirarattananon, S. B. Fuller, and R. J. Wood, "Controlled flight of a biologically inspired, insect-scale robot." *Science (New York, N.Y.)*, vol. 340, no. 6132, pp. 603–7, may 2013. [Online]. Available: http://www.ncbi.nlm.nih.gov/pubmed/23641114

[7] G. Loianno, G. Cross, C. Qu, Y. Mulgaonkar, J. A. Hesch, and V. Kumar, "Flying Smartphones: Automated Flight Enabled by Consumer Electronics," *IEEE Robotics & Automation Magazine*, vol. 22, no. 2, pp. 24–32, jun 2015. [Online]. Available: http://ieeexplore.ieee.org/document/7105372/

[8] H. Marvi, C. Gong, N. Gravish, H. Astley, M. Travers, R. L. Hatton, J. R. Mendelson, H. Choset, D. L. Hu, and D. I. Goldman, "Sidewinding with minimal slip: snake and robot ascent of sandy slopes." *Science (New York, N.Y.)*, vol. 346, no. 6206, pp. 224–9, oct 2014. [Online]. Available: http://www.ncbi.nlm.nih.gov/pubmed/25301625

[9] C. Li, P. B. Umbanhowar, H. Komsuoglu, D. E. Koditschek, and D. I. Goldman, "From the Cover: Sensitive dependence of the motion of a legged robot on granular media." *Proceedings of the National Academy of Sciences of the United States of America*, vol. 106, no. 9, pp. 3029–34, mar 2009. [Online]. Available: http://www.ncbi.nlm.nih.gov/pubmed/19204285 http://www.pubmedcentral.nih.gov/articlerender.fcgi?artid=PMC2637910

[10] J. Kumagai, "Sand trap," *IEEE Spectrum*, vol. 41, no. 6, pp. 44–50, jun 2004. [Online]. Available: http://ieeexplore.ieee.org/document/1303373/

[11] R. M. Nedderman, *Statics and kinematics of granular materials*. Cambridge University Press, 2005.

[12] C. Li, T. Zhang, and D. I. Goldman, "A terradynamics of legged locomotion on granular media," *Science*, vol. 339, no. 6126, pp. 1408–1412, Mar. 2013.

[13] ——, "A Terradynamics of Legged Locomotion on Granular Media," Tech. Rep. [Online]. Available: http://science.sciencemag.org/

[14] N. Gravish, P. B. Umbanhowar, and D. I. Goldman, "Force and Flow Transition in Plowed Granular Media," *Physical Review Letters*, vol. 105, no. 12, p. 128301, sep 2010. [Online]. Available: https://link.aps.org/doi/10.1103/PhysRevLett.105.128301

[15] T. Zhang, F. Qian, C. Li, P. Masarati, A. M. Hoover, P. Birkmeyer, A. Pullin, R. S. Fearing, and D. I. Goldman, "Ground fluidization promotes rapid running of a lightweight robot," *The International Journal of Robotics Research*, vol. 32, no. 7, pp. 859–869, jun 2013. [Online]. Available: http://journals.sagepub.com/doi/10.1177/0278364913481690

[16] F. Qian, T. Zhang, W. Korff, P. B. Umbanhowar, R. J. Full, and D. I. Goldman, "Principles of appendage design in robots and animals determining terradynamic performance on flowable ground," *Bioinspir. Biomim.*, vol. 10, no. 5, p. 056014, Oct. 2015.

[17] C. Li, S. T. Hsieh, and D. I. Goldman, "Multi-functional foot use during running in the zebra-tailed lizard (callisaurus draconoides)," *J. Exp. Biol.*, vol. 215, no. Pt 18, pp. 3293–3308, Sept. 2012.

[18] G. D. Canio, S. Stoyanov, J. C. Larsen, J. Hallam, A. Kovalev, T. Kleinteich, S. N. Gorb, and P. Manoonpong, "A robot leg with compliant tarsus and its neural control for efficient and adaptive locomotion on complex terrains," *Artificial Life and Robotics*, vol. 21, no. 3, pp. 274–281, sep 2016. [Online]. Available: http://link.springer.com/10.1007/s10015-016-0296-3

[19] Hyun-jin Kang, K. Hashimoto, H. Kondo, K. Hattori, K. Nishikawa, Y. Hama, Hun-ok Lim, A. Takanishi, K. Suga, and K. Kato, "Realization of biped walking on uneven terrain by new foot mechanism capable of detecting ground surface," in *2010 IEEE International Conference on Robotics and Automation*. IEEE, may 2010, pp. 5167–5172. [Online]. Available: http://ieeexplore.ieee.org/document/5509348/

[20] C. Piazza, C. Della Santina, G. M. Gasparri, M. G. Catalano, G. Grioli, M. Garabini, and A. Bicchi, "Toward an adaptive foot for natural walking," in *2016 IEEE-RAS 16th International Conference on Humanoid Robots (Humanoids)*. IEEE, nov 2016, pp. 1204–1210. [Online]. Available: http://ieeexplore.ieee.org/document/7803423/

[21] D. Mura, C. D. Santina, C. Piazza, I. Frizza, C. Morandi, M. Garabini, G. Grioli, and M. G. Catalano, "Exploiting Adaptability in Soft Feet for Sensing Contact Forces," *IEEE Robotics and Automation Letters*, vol. 5, no. 2, pp. 391–398, apr 2020.

[22] G. E. Weissengruber, G. F. Egger, J. R. Hutchinson, H. B. Groenewald, L. Elsässer, D. Famini, and G. Forstenpointner, "The structure of the cushions in the feet of African elephants (Loxodonta africana)." *Journal of anatomy*, vol. 209, no. 6, pp. 781–92, dec 2006. [Online]. Available: http://www.ncbi.nlm.nih.gov/pubmed/17118065 http://www.pubmedcentral.nih.gov/articlerender.fcgi?artid=PMC2048995

[23] S. Hauser, P. Eckert, A. Tuleu, and A. Ijspeert, "Friction and damping of a compliant foot based on granular jamming for legged robots," in *2016 6th IEEE International Conference on Biomedical Robotics and Biomechatronics (BioRob)*. IEEE, jun 2016, pp. 1160–1165. [Online]. Available: http://ieeexplore.ieee.org/document/7523788/

[24] S. Hauser, M. Mutlu, F. Freundler, and A. Ijspeert, "Stiffness Variability in Jamming of Compliant Granules and a Case Study Application in Climbing Vertical Shafts," in *2018 IEEE International Conference on Robotics and Automation (ICRA)*. IEEE, may 2018, pp. 1559–1566. [Online]. Available: https://ieeexplore.ieee.org/document/8462899/

[25] S. Hauser, M. Mutlu, P. Banzet, and A. Ijspeert, "Compliant universal grippers as adaptive feet in legged robots," *Advanced Robotics*, vol. 32, no. 15, pp. 825–836, aug 2018. [Online]. Available: https://www.tandfonline.com/doi/full/10.1080/01691864.2018.1496851

[26] D. I. Goldman and P. Umbanhowar, "Scaling and dynamics of sphere and disk impact into granular media," *Physical Review E*, vol. 77, no. 2, p. 021308, feb 2008. [Online]. Available: http://www.ncbi.nlm.nih.gov/pubmed/18352023 https://link.aps.org/doi/10.1103/PhysRevE.77.021308

[27] E. Brown, N. Rodenberg, J. Amend, A. Mozeika, E. Steltz, M. R. Zakin, H. Lipson, and H. M. Jaeger, "Universal robotic gripper based on the jamming of granular material," *Proceedings of the National Academy of Sciences*, vol. 107, no. 44, pp. 18 809–18 814, nov 2010. [Online]. Available: http://www.pnas.org/cgi/doi/10.1073/pnas.1003250107

[28] P. Umbanhowar and D. I. Goldman, "Granular impact and the critical packing state," *Physical Review E*, vol. 82, no. 1, p. 010301, jul 2010. [Online]. Available: https://link.aps.org/doi/10.1103/PhysRevE.82.010301

[29] W. W. Dickinson and J. D. Ward, "Low depositional porosity in eolian sands and sandstones, Namib Desert," *Journal of Sedimentary Research A: Sedimentary Petrology & Processes*, vol. 64 A, no. 2, pp. 226–232, 1994.

[30] I. Albert, P. Tegzes, B. Kahng, R. Albert, J. G. Sample, M. Pfeifer, A.-L. Barabási, T. Vicsek, and P. Schiffer, "Jamming and Fluctuations in Granular Drag," *Physical Review Letters*, vol. 84, no. 22, pp. 5122–5125, may 2000. [Online]. Available: https://link.aps.org/doi/10.1103/PhysRevLett.84.5122